

# Gluing and grazing bifurcations in periodically forced 2-dimensional integrate-and-fire models\*

Albert Granados<sup>†</sup> and Gemma Huguet<sup>‡</sup>

## Abstract

In this work we consider a general 2-dimensional integrate-and-fire model. Assuming that the system possesses an attracting node, we show that, when periodically driven, the system possesses a periodic orbit which may undergo tangent-grazing or nonsmooth-grazing bifurcation. For the former simulations show that the system can exhibit bi-stability. For the latter we perform a semi-rigorous study of the existence of periodic orbits. Instead of using the traditional *impact* map we use the stroboscopic one, which becomes a 2-dimensional piecewise-smooth discontinuous map. For some parameter values we are able to show that the map is a quasi-contraction and possesses a (locally) unique maximin periodic orbit.

**Keywords:** integrate-and-fire, piecewise-smooth maps, quasi-contractions.

## 1 Introduction

Integrate-and-fire systems are hybrid systems such that, when a certain condition is satisfied (the system reaches a certain threshold) a reset occurs. Such systems are widely used in neuroscience, as these resets represent neuron spikes. They can be seen as simplified versions of slow-fast systems, and the resets mimic large amplitude oscillations.

Examples of such systems range from simple one-dimensional models as the leaky integrate-and-fire, which models simple tonic spiking, to higher dimensional ones exhibiting more complicated behaviour. Examples of the former are systems with variable threshold to model type III excitability observed in the auditory brainstem [MHR12] or systems with adaptation variables [BG05].

---

\*This work has been partially supported by MINECO MTM2015-65715-P Spanish grant and Marie Curie FP7 COFUND Ørsted fellowship. We acknowledge the use of the UPC Dynamical Systems group's cluster for research computing (<https://dynamicalsystems.upc.edu/en/computing/>)

<sup>†</sup>algr@dtu.dk, Department of Applied Mathematics and Computer Science, Technical University of Denmark, Building 303B, 2800 Kgs. Lyngby, Denmark.

<sup>‡</sup>Department of Mathematics, Polytechnic University of Catalonia, Av. Diagonal 647, 08028 Barcelona, Spain.

A general framework to study the dynamics of such systems becomes very difficult to obtain, mainly because they are discontinuous due to the reset condition, even when the input current are assumed to be constant (they remain autonomous). In more realistic one considers periodic inputs instead. In this case, even one-dimensional integrate-and-fire systems exhibit very rich dynamics [KHR81, TFS02]. Recent works show how theory for nonsmooth systems can be used to obtain model-independent general results [GKC14, GK15]. However, these are limited to one-dimensional systems exhibiting simple subthreshold dynamics, as they are based on theory for circle maps (see [GAK16] for a recent review).

In this work we recover theoretical results from the 80's ([GT85, GGT84]) that may provide a theoretical background to understand the dynamics of more complicated integrate-and-fire systems. In particular we study 2-dimensional systems subject to a periodic forcing by means of the stroboscopic map, which becomes a 2-dimensional discontinuous map. By means of semi-rigorous numerical arguments we show that the stroboscopic map becomes a quasi-contraction possessing minimax unique periodic orbits.

## 2 General setting

### 2.1 System description

Let us consider the system

$$\begin{cases} \dot{x} = f(x, y) + I(t) \\ \dot{y} = g(x, y), \end{cases} \quad (1)$$

with  $(x, y) \in \mathbb{R}^2$ ,  $f$  and  $g$  smooth enough functions and  $I(t)$  a  $T$ -periodic function given by

$$I(t) = \begin{cases} A & \text{if } t \in (nT, nT + dT] \\ 0 & \text{if } t \in (nT + dT, (n+1)T]. \end{cases} \quad (2)$$

Let us also consider a *threshold* manifold  $\Theta$  in the  $\mathbb{R}^2$  given by

$$\Theta = \{(x, y) \in \mathbb{R}^2 \mid \theta(x, y) = 0\},$$

where  $\theta : \mathbb{R}^2 \rightarrow \mathbb{R}$  is a smooth function. We then submit system (1) to the following algebraic condition. Whenever a trajectory reaches the threshold  $\Theta$  at a certain time  $t = t_*$ , it is reset to a certain value:

$$\theta(x(t_*^-), y(t_*^-)) = 0 \longrightarrow \begin{cases} x(t_*^+) = x_r \\ y(t_*^+) = y(t_*^-) + \Delta \end{cases}, \quad (3)$$

$x_r, \Delta \in \mathbb{R}$ .

This can be written in terms of a reset map,

$$\mathfrak{R} : \begin{array}{ccc} \Theta & \longrightarrow & \mathbb{R}^2 \\ (x, y) & \longmapsto & (x_r, y + \Delta), \end{array} \quad (4)$$

which is applied whenever a trajectory collides with the threshold  $\Theta$ . When this occurs, we say that system (1)-(3) exhibits a spike.

Although, these spikes introduce discontinuities to the trajectories of system (1), the latter are all well defined, as one just needs to apply the map  $\mathfrak{R}$  whenever the threshold is reached.

We define the subthreshold domain as

$$\mathbb{D} = \{(x, y) \in \mathbb{R}^2, | x > x_r, \theta(x, y) > 0, x < x_{\max}\},$$

for some  $x_{\max} > 0$ . Given  $z \in \mathbb{D}$ , we will call  $\phi(t; z)$  the solution of the system such that  $\phi(0; z) = z$ . If  $z \in \mathbb{D}$ , we will say that its trajectory is subthreshold if  $\phi(t; z) \in \mathbb{D}$  for all  $t \geq 0$ . In particular, an invariant set is subthreshold if it is contained in  $\Theta$ .

We now assume that, for  $A = 0$ , system (1)

*H.1* possesses an attracting equilibrium point  $(x^*, y^*) \in \mathbb{D}$  of the node type,

*H.2* for any  $(x, y) \in \mathbb{D}$ , trajectories do not exhibit spikes.

## 3 Stroboscopic map

### 3.1 Definition

Typically, systems with resets such as (1)-(3) are studied by means of the *firing* map: a Poincaré map onto the threshold  $\Theta$ . Although this provides a smooth map, the periodic forcing  $I(t)$  requires the explicit knowledge of the firing times in order to study periodic orbits. In this approach, we follow [GKC14] and consider the stroboscopic map instead:

$$\mathfrak{s}(z) = \phi(T; z),$$

where  $z = (x, y)$  and  $\phi(t; z)$  is the solution of system (1)-(3) such that  $z = \phi(0; z)$ . Note that system (1)-(3) is not autonomous and, hence, the stroboscopic map depends on the initial time,  $t_0$ . However, as we are interested in studying periodic orbits, we can assume from now on that  $t_0 = 0$ .

Depending on the number of spikes exhibited by a solution  $\phi(t; z)$  for  $t \in [0, T]$ , the stroboscopic map becomes a different combination of smooth maps given by integrating Eq. (1) and applying the reset map (4). Hence this is a piecewise-smooth map. To see this in more detail, let us define the sets

$$S_n = \left\{ z \in \mathbb{D} \mid \phi(t; z) \text{ reaches } n \text{ times} \right. \\ \left. \text{the threshold } \Theta \text{ for } 0 \leq t \leq T \right\}, \quad n \geq 0. \quad (5)$$

In this work we will mainly focus on the existence of periodic orbits and their bifurcations involving the sets  $S_0$  and  $S_1$ . We first see how to define  $\mathfrak{s}$  in these sets. We refer to Figure 1 in order to illustrate what follows.

If  $z \in S_0$ , no spikes occur and  $\mathfrak{s}(z)$  becomes



be extended to all points in  $\mathbb{D}$  whose flow  $\varphi_A(t; x, y)$  reaches the threshold for some  $t^* > 0$ , independently on whether  $t^* \leq dT$  or not.

The map  $\mathfrak{R}$  is the reset map defined in (4) carrying on time. The map  $\tilde{P}_2$  integrates the flow with initial condition at the reset manifold  $R$  for the remaining time until  $t = dT$ . Note that, similarly as for  $P_1$ ,  $\tilde{P}_2$  can also be extended outside its natural domain by letting  $t < 0$ . Finally, the map  $P_3$  is a truly stroboscopic map, which integrates the flow  $\varphi_0$  for fixed time  $T - dT$ .

Recalling condition *H.2*, spikes are only possible for  $A > 0$  ( $0 \leq t^* \leq dT$ ). Hence, for  $z \in S_1$ , the stroboscopic map becomes

$$\mathfrak{s}(z) = \mathfrak{s}_1(z) := P_3 \circ \tilde{P}_2 \circ \tilde{\mathfrak{R}} \circ P_1(z). \quad (10)$$

Then, the stroboscopic map restricted to  $S_0 \cup S_1$  becomes

$$\mathfrak{s}(z) = \begin{cases} \mathfrak{s}_0(z) & \text{if } z \in S_0 \\ \mathfrak{s}_1(z) & \text{if } z \in S_1. \end{cases}$$

By considering  $\tilde{P}_1$  and  $\tilde{P}_3$  the extended versions (to  $\mathbb{R}^2 \times \mathbb{T}_T$ ) of the maps  $P_1$  and  $P_3$  and recalling that spikes occur for  $0 \leq t \leq dT$ , if  $z \in S_n$  the stroboscopic map becomes the piecewise-smooth map

$$\mathfrak{s}(z_0) = \tilde{P}_3 \circ \tilde{P}_2 \circ \left( \tilde{\mathfrak{R}} \circ \tilde{P}_1 \right)^n (z_0). \quad (11)$$

**Remark 1.** *If one allows the system to exhibit spikes for  $A = 0$ , then the stroboscopic map can be similarly defined by accordingly reordering in Equation (11) the sequence of maps  $\tilde{P}_i$  and  $\tilde{\mathfrak{R}}$ .*

**Remark 2.** *The stroboscopic map is discontinuous even if one identifies the threshold and the reset manifolds:  $\Theta \sim R$ . Although this would make trajectories of the flow continuous, the field (1) does not necessary coincide at the manifolds  $\Theta$  and  $R$  and hence the map would still be discontinuous.*

Let us now study the border,  $\Sigma_1$ , that separates the sets  $S_0$  and  $S_1$  and hence becomes a switching manifold of the stroboscopic map  $\mathfrak{s}$ . This border is formed by the union of points whose trajectories graze the threshold manifold  $\Theta$ . Such a grazing can occur in two different ways defining two different types of points in  $\Sigma_1$  :

- i) Tangent Grazing: points whose trajectory is tangent to  $\Theta$
- ii) Non-smooth Grazing: points whose trajectory is transversal to  $\Theta$  exactly for  $t = dT$ .

Note that non-smooth grazing occurs for  $t = dT$  and  $t = T = 0 \bmod T$ , at times when the pulse  $I(t)$  is enabled or disabled. Provided that trajectories can only reach the threshold when  $A > 0$ , (condition *H.2*), non-smooth grazing can only occur at points of the form  $\phi(dT; (x, y))$ . However, trajectories may exhibit tangent grazing for  $0 < t < dT$ .

As mentioned above, the switching manifold  $\Sigma_1$  can be split in two pieces according to *i*) and *ii*):

$$\Sigma_1 = \Sigma_1^{\text{Tan}} \cup \Sigma_1^{\text{Tran}},$$

where

$$\begin{aligned} \Sigma_1^{\text{Tan}} = \Big\{ z \in \mathbb{D} \mid z = \varphi_A(t; z), t \in [0, t^*], \theta(\varphi_A(t^*; z)) = 0, \\ \nabla \theta(\varphi_A(t^*; z)) \cdot \varphi_A(t^*; z) = 0 \Big\}, \end{aligned}$$

and

$$\Sigma_1^{\text{Tran}} = \{ z \in \mathbb{D} \mid \theta(\varphi_A(dT; z)) = 0 \},$$

**Remark 3.** Similarly, one can define boundaries  $\Sigma_i^{\text{Tan}}$  and  $\Sigma_i^{\text{Tran}}$  with  $i > 1$ , which separate sets exhibiting more than one spike.

**Remark 4.** The boundary  $\Sigma^{\text{Tan}}$  contains a piece of the trajectory which is tangent to  $\Theta$  for  $I = A$  (constant). Hence, if a point  $z \in S_1$  spikes tangentially, then it belongs to  $\Sigma^{\text{Tan}}$ , and all points  $S_1 \setminus \left( \bigcup_{i \geq 1} \Sigma_i^{\text{Tan}} \right)$  spike transversally.

### 3.2 Virtual extension and contractiveness of the stroboscopic map

The maps  $\mathfrak{s}_0$  and  $\mathfrak{s}_1$  can in some cases be extended to their “virtual” domains,  $S_1$  and  $S_0$ , respectively.

Clearly, by ignoring the reset condition, one can always smoothly extend  $\mathfrak{s}_0$  to  $S_1$ . That is, if  $z \in S_1$ , then we extend  $\mathfrak{s}_0$  to  $z$  by setting  $\mathfrak{s}_0(z) = \varphi_0(t - dT; \varphi_A(dT; z))$ , which is well defined.

Under certain conditions, one can also extend the map  $\mathfrak{s}_1$  to  $S_0$ . Let  $z \in S_0$  and assume that there exists  $t^* > dT$  such that  $\varphi_A(t^*; z) \in \Theta$ . Then, although  $z \notin S_1$ ,  $\mathfrak{s}_1$  is also well defined at such a point by letting  $t^* > dT$  in  $P_1$  and using  $t > dT$  when applying the map  $\tilde{P}_2$ , which will consist of integrating backwards a time  $|dT - t^*|$  the flow  $\varphi_A$ . Note that, if  $z \in S_0$  is close to  $\Sigma_1^{\text{Tan}}$ , then it may be that such  $t^*$  does not exist and hence one cannot extend  $\mathfrak{s}_1$  to  $S_0$ .

Let us assume that the flows  $\varphi_A$  and  $\varphi_0$  are contracting in  $\mathbb{D}$ . Clearly, this implies that  $\mathfrak{s}_0$  is a contracting map, even when extended to  $S_1$ . The spikes exhibited by trajectories of points in  $S_1$  may introduce expansiveness to  $\mathfrak{s}_1$ . However, if  $dT \ll T$  then  $T - dT$  may be large enough to compensate such expansions when flowing  $\varphi_0$ .

### 3.3 Differential of the stroboscopic map

We now compute the differential of  $\mathfrak{s}$  in  $S_0$  and  $S_1$ ,  $D\mathfrak{s}_0$  and  $D\mathfrak{s}_1$ . This will be used to compute fixed points through a Newton method and their stability. On one hand  $\mathfrak{s}_0$  becomes the composition of two stroboscopic maps. Provided that

$I(t)$  is a piecewise-constant function, its Jacobian matrix of the stroboscopic map can be computed by solving the variational equations

$$\dot{\delta}_A = \begin{pmatrix} \frac{\partial}{\partial x} f(\varphi_A(t; z)) & \frac{\partial}{\partial y} f(\varphi_A(t; z)) \\ \frac{\partial}{\partial x} g(\varphi_A(t; z)) & \frac{\partial}{\partial y} g(\varphi_A(t; z)) \end{pmatrix} \delta_A \quad (12)$$

where

$$\delta_A = \begin{pmatrix} \frac{\partial}{\partial x} \Pi_x(\varphi_A(t; z)) & \frac{\partial}{\partial y} \Pi_x(\varphi_A(t; z)) \\ \frac{\partial}{\partial x} \Pi_y(\varphi_A(t; z)) & \frac{\partial}{\partial y} \Pi_y(\varphi_A(t; z)) \end{pmatrix}.$$

Equation (12) must be integrated along the flow  $\varphi_A(t; z)$  using the identity matrix as initial condition.

Hence, for  $z \in S_0$ , we have

$$D\mathfrak{s}(z) = \delta_0(T - dT; \varphi_A(dT; z)) \cdot \delta_A(dT; z). \quad (13)$$

On the other hand, we compute the differential  $D\mathfrak{s}_1$  recalling its definition in Equation (10). We need then to take into account that the firing time,  $t^*$ , depends on the initial conditions. In order to compute  $Dt^*$  we apply the implicit function Theorem to the equation

$$F(t, x, y) = \theta(\varphi_A(t; (x, y))) = 0. \quad (14)$$

Let  $(t^*, x, y)$  be a solution of Eq. (14); that is,  $\varphi_A(t^*; (x, y)) \in \Theta$ . Then, assuming that

$$\frac{\partial}{\partial t} \theta(\varphi_A(t; (x, y)))|_{t=t^*} \neq 0, \quad (15)$$

we get

$$Dt(x, y) = - \frac{\nabla \theta(x, y) \cdot \delta_A(t^*)}{\nabla \theta(\varphi_A(t^*; (x, y))) \cdot \begin{pmatrix} f(x, y) \\ g(x, y) \end{pmatrix}}.$$

Note that condition (15) is equivalent to requiring that the flow is not tangent to  $\Theta$  at  $\varphi_A(t^*, (x, y))$ , and hence this is only valid when the spike is given by a transversal crossing between the flow and  $\Theta$ .

Then, the differentials of the maps (6)–(9)

$$\begin{aligned} DP_1(x, y) &= \begin{pmatrix} \delta_a(t^*) \\ Dt(x, y) \end{pmatrix} \\ D\tilde{\mathfrak{R}}(x, y, t) &= \begin{pmatrix} 0 & 0 & 0 \\ 0 & 1 & 0 \\ 0 & 0 & 1 \end{pmatrix} \\ D\tilde{P}_2(x, y, t) &= \begin{pmatrix} \delta_A(dT - t) & -f(x, y) \\ -g(x, y) \end{pmatrix} \\ DP_3(x, y) &= \delta_0(T - dT). \end{aligned}$$

Hence we get,

$$D\mathfrak{s}_1(x, y) = DP_r(x_2, y_2)D\tilde{P}_2(x_r, y_r, t_1)D\tilde{\mathfrak{R}}(x_1, y_1, t_1)DP_1(x, y),$$

where

$$(x_1, y_1, t_1) = P_1(x, y) \quad (x_r, y_r, t_1) = \tilde{\mathfrak{R}}(x_1, y_1, t_1) \quad (x_2, y_2) = \tilde{P}_2(x_r, y_r, t_1).$$

## 4 Bifurcations of fixed points

Recalling assumption *H.1*, for  $A = 0$ , system (1)-(3) possesses an attracting subthreshold equilibrium point of the node type,  $(x^*, y^*) \in \mathbb{D}$ . Although the periodic forcing  $I(t)$  is not continuous in  $t$ , averaging theorem [BM61] holds, as the system is Lipschitz in  $x$  and  $y$ . This implies that, when  $A > 0$  is small enough, system (1)-(3) possesses a  $T$ -periodic orbit, which is not differentiable at  $t = 0 \pmod{T}$  and  $t = dT \pmod{T}$ . When  $A$  is further increased, this periodic orbit undergoes a *grazing bifurcation* if it collides with the boundary  $\Theta$ . When this occurs, the stroboscopic map, possesses a fixed point  $\bar{z} \in S_0$  undergoing a *border collision bifurcation* when colliding with  $\Sigma_1$ . Following *i)* and *ii)* of Section 3.1, we distinguish two different types of bifurcations:

Bif.1 Tangent grazing bifurcation: the periodic orbit grazes tangentially  $\Theta$ , and the fixed point collides with  $\Sigma_1^{\text{Tan}}$ ,

Bif.2 Non-smooth grazing bifurcation: the periodic orbit grazes  $\Theta$  at the non-differentiable point given by  $t = dT$ , and the fixed points collides with  $\Sigma_1^{\text{Tran}}$ .

These two different situations may lead to different dynamics after the bifurcation. However, in this article we mainly focus in the second case, the non-smooth grazing case.

### 4.1 Border collision with $\Sigma_1^{\text{Tran}}$

Assume that the fixed point of  $\mathfrak{s}_0$  crosses transversally  $\Sigma^{\text{Tran}}$  for some parameter value and undergoes a border collision bifurcation. In this situation  $\mathfrak{s}$  may posses periodic orbits stepping both at  $S_0$  and  $S_1$ . We now introduce symbolic dynamics and some definitions in order to characterize such periodic orbits.

**Definition 1.** Given  $z \in S_0 \cup S_1$ , we define the itinerary of  $z$  by  $\mathfrak{s}$  as

$$I_{\mathfrak{s}}(z) = (a(z), a(\mathfrak{s}(z), a(\mathfrak{s}^2(z)), \dots)),$$

where

$$a(x) = \begin{cases} \mathcal{R} & \text{if } x \in S_1 \\ \mathcal{L} & \text{if } x \in S_0. \end{cases}$$



**Definition 2.** We call  $W_{p,q}$  the set of periodic symbolic sequences generated by a symbolic block of length  $q$  containing  $p$  symbols  $\mathcal{R}$ :

$$W_{p,q} = \left\{ \mathbf{y} \in \{\mathcal{L}, \mathcal{R}\}^{\mathbb{N}} \mid \mathbf{y} = \mathbf{x}^\infty, \mathbf{x} \in \{\mathcal{L}, \mathcal{R}\}^q \text{ and } \mathbf{x} \text{ contains } p \text{ symbols } \mathcal{R} \right\}$$

**Definition 3.** We say that a symbolic sequence  $\mathbf{x} \in W_{p,q}$  is maximin if

$$\min_{0 \leq k \leq q} (\sigma^k(\mathbf{x})) = \max_{\mathbf{y} \in W_{p,q}} \left( \min_{0 \leq k \leq q} (\sigma^k(\mathbf{y})) \right),$$

Alternatively, maximin itineraries can be defined as those belonging to the Farey tree of symbolic sequences (see [GAK16] for a recent review). Then, we may apply the following result:

**Theorem 1** (Dynamics of quasi-contractions). *Assume that there exist sets  $E_0 \subset S_0$  and  $E_1 \subset S_1$  s. t.*

- i)  $\mathfrak{s}(E_i) \subset E_0 \cup E_1$*
- ii)  $\mathfrak{s}_0$  and  $\mathfrak{s}_1$  contract in  $E_0$  and  $E_1$ , respectively.*
- iii)  $\mathfrak{s}^n(\Sigma^{Tran}) \cap \Sigma^{Tran} = \emptyset$  for all  $n \geq 1$ .*

*Then, provided that  $\mathfrak{s}$  preserves orientation,  $\mathfrak{s}$  possesses 0 or 1 periodic orbits. In the latter case, its itinerary is maximin.*

The previous result was stated in [GT88] for quasi-contractions in metric spaces and adapted in [GAK16] for piecewise-smooth contracting maps in  $\mathbb{R}^n$ .

## 4.2 Border collision with $\Sigma^{\text{Tan}}$

Unlike in the previous case, there is very little general theory that one can use to predict what are the actual dynamics of the system after a periodic orbit undergoes a tangent grazing bifurcation. This is typically done by studying the linearization of the Poincaré map [dBBC01, NK06, Nor97]. There exists a large literature in this directions devoted to nonsmooth systems such as impact oscillators [Nor01, DN00, DZ05, ZD06, TD06], hybrid systems [DH04] or linear normal form maps [Kow05, Sim14]. Such bifurcation plays also an important role in sliding dynamics [MdB04]. In this case, some authors have been recently able to prove the existence of bi-stability by reducing the dynamics to one-dimensional maps [GKN12, GKN16]. However, as in our case the system is non-autonomous and does not exhibit sliding. General statements are left for future work. In Section 5 we show through an example that, when the fixed point bifurcates by colliding with  $\Sigma_1^{\text{Tan}}$  then bi-stability may occur.

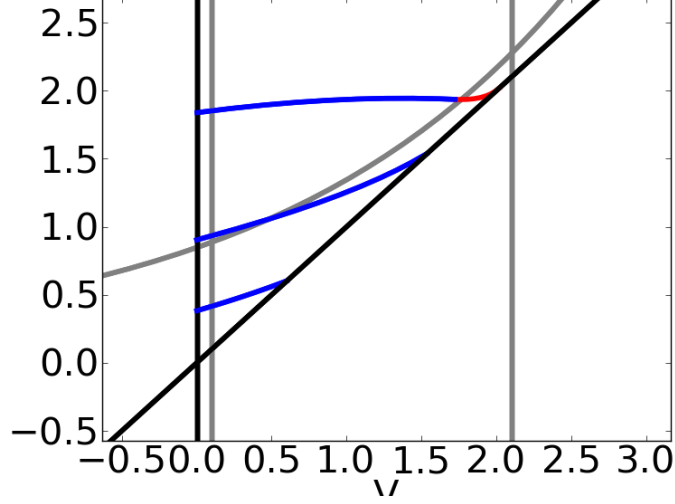


Figure 2: Boundaries  $\Sigma_1$ ,  $\Sigma_2$  and  $\Sigma_3$  (from top to bottom) for system (16) with  $c = 0.53$ ,  $V_r = 0.1$ ,  $A = 2$ ,  $\tau = 2$ ,  $T = 3$  and  $b = 0.5$ . In blue  $\Sigma^{\text{Tran}}$  and red  $\Sigma^{\text{Tan}}$ . In gray the nullclines for  $I = 0$  and  $I = A$ .

## 5 Numerical results

In this section we consider the system proposed in [MHR12] submitted to periodic forcing  $I(t)$  as in Equation (2):

$$\begin{aligned}\dot{V} &= -V + V_{\text{rest}} + I(t) \\ \tau_{\theta} \dot{\theta} &= -(\theta - \theta_{\infty}(V))\end{aligned}\tag{16}$$

being  $(V, \theta) \in \mathbb{R}^2$ ,  $\theta_{\infty}(V) = a + e^{b(V-c)}$  and the reset rule

$$\text{if } V(t) = \theta(t) \text{ then } V(t^+) = V_r \text{ and } \theta(t^+) = \theta(t^-) + \Delta.$$

System (16) is of the form of the general system (1), with and threshold manifold

$$\Theta = \{(V, \theta), | V - \theta = 0\}$$

subthreshold domain

$$\mathbb{D} = \{(V, \theta), | V \geq 0, V \leq \theta\}$$

and the reset map

$$\mathfrak{R} : \begin{array}{ccc} \Theta & \longrightarrow & R \\ (V, \theta) & \longmapsto & (V_r, \theta + \Delta). \end{array}$$

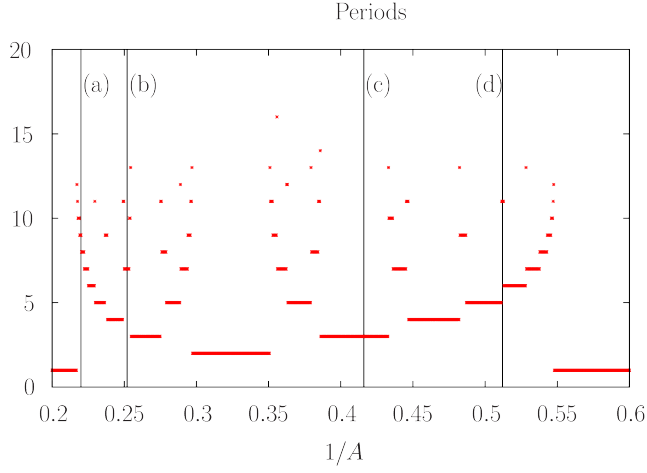


Figure 3: Periods of the periodic orbits found by direct simulation. Parameter values are  $c = 0.53$ ,  $V_r = 0.1$ ,  $A = 2$ ,  $\tau = 2$ ,  $T = 3$  and  $b = 0.1$ .

For  $A = 0$ , system (16) possesses an equilibrium point at  $(V^*, \theta^*) = (V_{\text{rest}}, \theta_\infty(V_{\text{rest}}))$  which is an attracting node. We assume  $(V^*, \theta^*) \in \mathbb{D}$  and we automatically get  $(V^*, \theta^*) \in \mathbb{D} \cap S_0$ .

As argued in Section 4, if  $(V^*, \theta^*) \in \mathbb{D}$ , then, for  $A > 0$  small enough, system (16) possesses a periodic orbit of amplitude  $O(A)$ . We then distinguish between two situations, depending on the parameters  $a$ ,  $b$  and  $c$ :

1.  $\theta_\infty(V) > V$  for all  $V > 0$ ,
2.  $\theta_\infty(V) < V$  for some  $V > 0$ .

These two situations do not only benefit different type of dynamics, but also model different spiking behaviours.

In the first case, the  $\theta$ -nullcline always stays in the subthreshold domain. As a consequence, the system possesses an attracting node for any value of  $I = A$  (constant). This situation benefits the corresponding periodic orbit to bifurcate through tangent sliding described in Section 4.2.

In the second case, the  $\theta$ -nullcline crosses the threshold. When this occurs, the system may possess a virtual attracting equilibrium for some values of  $I = A$  (constant). This makes trajectories be faster pushed towards the threshold hence benefiting non-smooth grazing bifurcation for the corresponding periodic orbit described in Section 4.1.

In this work we will mainly focus in the second situation. In Figure 3 we show the periods of the periodic orbits found by direct simulation when varying  $A$ . They follow period adding-like structures, which suggests that they itineraries are maximin (see [GAK16] for more details). To study this in more rigorously, we perform an algorithm in order to numerically find sets  $E_i$  of Theorem 1. We

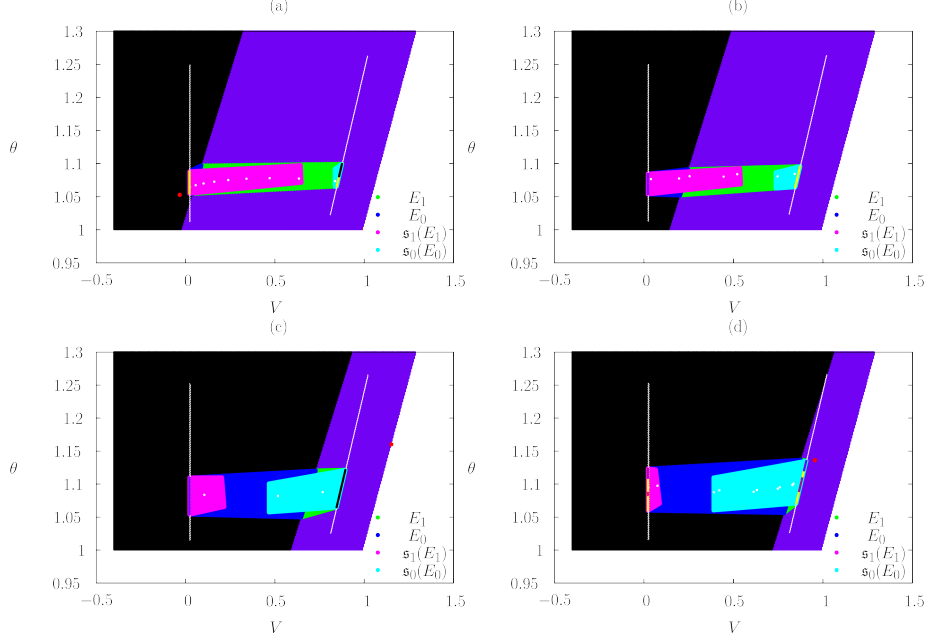


Figure 4: Sets  $E_i$  of Theorem 1 for the parameter values labeled in Figure 3. White points are the periodic orbit found by direct simulation. Red point is a virtual fixed point found by extending the maps  $\mathfrak{s}_i$  in their virtual domains, as explained in Section 3.2. Black background is  $S_0$ , blue background is  $S_1$ . Blue and green sets are  $E_0$  and  $E_1$ , respectively. Pink and light blue are  $\mathfrak{s}_1(E_1)$  and  $\mathfrak{s}_0(E_0)$ , respectively. The white lines are the images  $\mathfrak{s}_0(\Sigma_1)$  and  $\mathfrak{s}_1(\Sigma_1)$ . Colored lines are the images of  $\sigma$  (see text) by  $\mathfrak{s}_i$ . Those segments that stay connected for all iterates of  $\mathfrak{s}$  are plotted with the same color.

first get a small segment  $\sigma \subset \Sigma_1$  “close” to the periodic orbit found by direct simulation. This segment is iterated by  $\mathfrak{s}_0$  and  $\mathfrak{s}_1$ . We then consider the two polygons formed by the segments  $\sigma$  and  $\mathfrak{s}_0(\sigma)$ , and  $\sigma$  and  $\mathfrak{s}_1(\sigma)$  (see Figure 4). We then check whether the images of these polygons is contained in their union. As the map is contracting, the union of these polygons forms a convex polygon, which makes it easy to check this inclusion. If any of the images is not contained in the union, then we enlarge the initial segment  $\sigma$  in the direction that failed and we check again. If at some point we succeed, then we have found sets  $E_i$  satisfying *i*) and *ii*) of Theorem 1. For all parameter values of  $A$  appearing in Figure 3 we have been able to find such sets. It remains to see whether *iii*) holds. This is done by checking whether all points in  $\sigma$  visit the  $S_0$  and  $S_1$  altogether or not. In Figure 5 we show examples of values of  $A$  for which condition *iii*) is satisfied (Figures (b) and (c)) and not satisfied (Figure (a) and (d)). For parameter values corresponding to (b) and (c) we have hence been able to

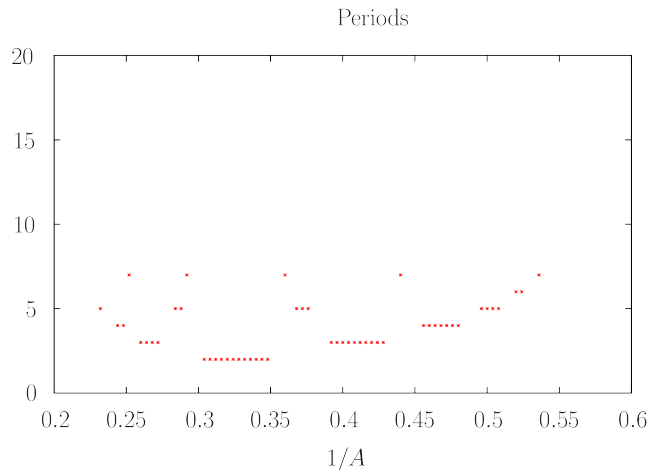


Figure 5: Periodic orbits satisfying conditions of Theorem 1.

prove semi-rigorously the existence of a unique periodic orbit whose symbolic dynamics is maximin, provided that the hypothesis of Theorem 1 are checked numerically.

We now consider the situation described in Section 4.2. For  $b = 0.6$  we find that the periodic orbit obtained by periodically forcing the attracting fixed point  $(V^*, \theta^*)$  bifurcates tangentially (see Figure 6). In this case we are not able to check the conditions of Theorem 1. Moreover, as one can see in Figure 6 there exists bi-stability, as we find coexisting fixed points in  $S_0$  and  $S_1$  around  $1/A = 0.65$ .

Future work will be devoted to study the viability of the application of the techniques developed in [GKN12] to this case.

## References

- [BG05] R. Brette and W. Gerstner. Adaptive exponential integrate-and-fire model as an effective description of neuronal activity. *J. Neurophysiol.*, 94:3637–3642, 2005.
- [BM61] N.N. Bogoliubov and Y.A. Mitropolski. *Asymptotic methods in the theory of non-linear oscillations*. Gordon and Breach, 1961.
- [dBBC01] M. di Bernardo, C. J. Budd, and A. R. Champneys. Normal form maps for grazing bifurcations in  $n$ -dimensional piecewise-smooth dynamical systems. *Physica D*, 160(3-4):222–254, 2001.
- [DH04] V. Donde and I.A. Hiskens. Grazing bifurcations in periodic hybrid systems. volume 4, pages 697–700, 2004.

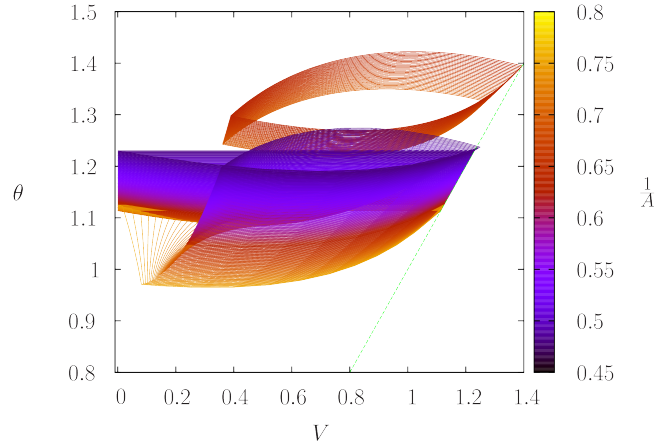


Figure 6: Periodic orbits for different values of  $A$ . There exist coexistence between a spiking and a non-spiking one. Parameter values:  $b = 0.6$  and  $T = 3$ . The rest as in Figure 3.

- [DN00] H. Dankowicz and A. B. Nordmark. On the origin and bifurcations of stick-slip oscillations. *Physica D: Nonlinear Phenomena*, 136(3-4):280–302, 2000.
- [DZ05] H. Dankowicz and X. Zhao. Local analysis of co-dimension-one and co-dimension-two grazing bifurcations in impact microactuators. *Physica D*, 202:238–257, 2005.
- [GAK16] A. Granados, Ll. Alsedà, and M. Krupa. The period adding and incrementing bifurcations: from rotation theory to applications. *SIAM Review*, 2016. Accepted for publication.
- [GGT84] J.-M. Gambaudo, P. Glendinning, and C. Tresser. Collage de cycles et suites de Farey. *C. R. Acad. Sc. Paris, série I*, 299:711–714, 1984.
- [GK15] A. Granados and M. Krupa. Firing-rate, symbolic dynamics and frequency dependence in periodically driven spiking models: a piecewise-smooth approach. *Nonlinearity*, 28:1163–1192, 2015.
- [GKC14] A. Granados, M. Krupa, and F. Clément. Border collision bifurcations of stroboscopic maps in periodically driven spiking models. *SIAM J. Appl. Dyn. Syst.*, 13(4):1387–1416, 2014.
- [GKN12] P. Glendinning, P. Kowalczyk, and A.B. Nordmark. Attractors near grazing-sliding bifurcations. *Nonlinearity*, 25:1867–1885, 2012.
- [GKN16] P. Glendinning, P. Kowalczyk, and A.B. Nordmark. Multiple attractors in grazing-sliding bifurcations in filippov-type flows. *IMA Journal of Applied Mathematics*, 2016.

- [GT85] J.-M. Gambaudo and C. Tresser. Dynamique régulière ou chaotique. applications du cercle ou de l'intervalle ayant une discontinuité. *C. R. Acad. Sc. Paris, série I*, 300:311–313, 1985.
- [GT88] J.-M. Gambaudo and C. Tresser. On the dynamics of quasi-contractions. *BOL. SOC. BRAS. MAT.*, 19:61–114, 1988.
- [KHR81] J.P. Keener, F.C Hoppensteadt, and J. Rinzel. Integrate-and-fire models of nerve membrane response to oscillatory input. *SIAM J. Appl. Dyn. Syst. (SIADS)*, 41:503–517, 1981.
- [Kow05] P. Kowalczyk. Robust chaos and border-collision bifurcations in non-invertible piecewise-linear maps. *Nonlinearity*, 18(2):485, 2005.
- [MdB04] P. Kowalczyk M. di Bernardo, A. R. Champneys. Corner collision and grazing sliding: practical examples of border collision bifurcations. In F. Vestroni G. Rega, editor, *Chaotic Dynamics and Control of Systems and Processes in Mechanics*. Kluwer Academic, Holland, 2004.
- [MHR12] X. Meng, G. Huguet, and J. Rinzel. Type III excitability, slope sensitivity and coincidence detection. *Disc. Cont. Dyn. Syst.*, 32:2720–2757, 2012.
- [NK06] A. Nordmark and P. Kowalczyk. A codimension-two scenario of sliding solutions in grazing-sliding bifurcations. *Nonlinearity*, 19:1–26, 2006.
- [Nor97] A. B. Nordmark. Universal limit mapping in grazing bifurcations. *Phys. Rev. E*, 55(1):266–270, 1997.
- [Nor01] A. B. Nordmark. Existence of periodic orbits in grazing bifurcations of impacting mechanical oscillators. *Nonlinearity*, 14(6):1517, 2001.
- [Sim14] D.J.W. Simpson. Sequences of periodic solutions and infinitely many coexisting attractors in the border-collision normal form. *Int. J. Bifurcation and Chaos*, 24, 2014.
- [TD06] P. Thota and H. Dankowicz. Continuous and discontinuous grazing bifurcations in impacting oscillators. *Physica D*, 214:187–197, 2006.
- [TFS02] P.H.E. Tiesinga, J.-M. Fellous, and T.J. Sejnowski. Spike-time reliability of periodically driven integrate-and-fire neurons. *Neurocomputing*, 44:195–200, 2002.
- [ZD06] X. Zhao and H. Dankowicz. Unfolding degenerate grazing dynamics in impact actuators. *Nonlinearity*, 19:399–418, 2006.